

Novel Vortex Solid State in $\text{YBa}_2\text{Cu}_3\text{O}_{7-\delta}$ Twinned Crystals.

B. Maiorov, and E. Osquiguil

Centro Atómico Bariloche and Instituto Balseiro,
Comisión Nacional de Energía Atómica, 8400 S. C. de Bariloche, R. N., Argentina.
 (November 1, 2018)

We report on the scaling of transport properties around the vortex melting in $\text{YBa}_2\text{Cu}_3\text{O}_{7-\delta}$ oriented-twin single crystals in applied magnetic fields between 1T and 18T. We find that for all the measured field range the linear resistivity scales as $\rho(t, \theta) \sim t^{sy} \mathcal{F}_{\pm}(\sin(\theta)t^{-sx})$, with $t = |T - T_{BG}|$ and θ the angle between de planar defects and the magnetic field. The scaling is valid only for angles where the transition temperature $T_{BG}(\theta)$ shows a cusp. The critical exponents sx and sy are in agreement with the values predicted by Lidmar and Wallin only at magnetic fields below 4T. A change in the value of sx from $sx = 1 \pm 0.2$ to $sx = 3 \pm 0.2$ at around $H^{cr} \approx 4\text{T}$ when the magnetic field is increased, is responsible for changes in the shape of the $T_{BG}(\theta)$ curve and in the dependence of the linear dissipation on temperature and angle. The results strongly suggest the existence of a different vortex glassy phase in twinned crystals compared to the Bose-glass state found in samples with linear defects.

One of the most important aspects in high temperature superconductors is the existence of a melting line in the magnetic field-temperature ($H - T$) vortex phase diagram. The quest to understand the thermodynamic nature of the transition has been reflected in an important number of publications.¹ Nowadays it is accepted that in clean crystals the solid-liquid transition is first order, while the introduction of random point-like or correlated disorder transforms it into second order. Due to the high value of the Ginsburg parameter in high T_c materials, the critical region associated with this kind of transition becomes experimentally accessible. This important fact has led to the development of scaling theories^{2,3} which describe the vortex dynamics near the transition, enclosing its properties into two critical exponents. In both theories the critical exponents settle the way in which, the correlation length, $\xi \sim |T - T_{BG}|^{-\nu} = t^{-\nu}$, and the time scale in which a fluctuation of this size survives, $\tau \sim \xi^z$, diverge as the transition is approached. In the Bose-glass theory *linear* correlated defects induce an anisotropic correlation volume³ with $\xi_{\parallel} \sim \xi_{\perp}^2$ which are, respectively, the correlation lengths parallel and perpendicular to the correlated defects. In this theory³ the linear resistivity is predicted to scale as

$$\rho(t, \theta) \sim t^{sy} \mathcal{F}_{\pm}(\sin(\theta)t^{-sx}) \quad (1)$$

with a phase boundary separating the Bose-glass and the vortex liquid of the form

$$T_{BG}(\theta) = T_{BG}(0) \left[1 - \left(\frac{\sin(\theta)}{x_c} \right)^{1/sx} \right] \quad (2)$$

where $sy = \nu(z - 2)$, $sx = 3\nu$, and $x_c = \sin(\theta_c)t^{sx}$. Lidmar and Wallin pointed out⁴ that the correct thermodynamic variable to be included in the scaling anzats for the dynamical response of the vortex system in tilted magnetic fields is \mathbf{B} , instead of \mathbf{H} as used in ref.³. This

important remark leads to a modification of eqs. 1 and 2 through a change in the dependence of sx on the critical exponent ν .^{4,5} Accordingly, the form of the new phase boundary is given by eq. 2 with $sx = \nu$, while the linear resistivity still scales as eq. 1 but again with $sx = \nu$.

Equation 2 describes one of the key characteristics of the Bose-glass to liquid transition, *i.e.* the existence of a cusp in the transition curve at $\theta = 0$. This cusp was first observed by Worthington *et al.*⁶ in twinned $\text{YBa}_2\text{Cu}_3\text{O}_{7-\delta}$ crystals. Fleshler *et al.*⁷ studied the vortex dynamics for different orientations of the twin boundaries with respect to the applied field and current, and explained the cusp in terms of pinning effects by the twin potentials. The relation between the cusp and the Bose-glass transition was shown by Jiang *et al.*⁸ through transport measurements in $\text{YBa}_2\text{Cu}_3\text{O}_{7-\delta}$ crystals with columnar defects. Later on, Grigera *et al.*⁹ identified a Bose-glass phase in twinned $\text{YBa}_2\text{Cu}_3\text{O}_{7-\delta}$ crystals through a scaling analysis of the vortex dynamics near the cusp line. An interesting point related to the shape of the cusp, however, has gone unnoticed in the literature. While in samples with columnar defects the transition curve is well described by $T_{BG}(\theta) \sim 1 - |\theta|$ at small angles,^{8,10,11} in twinned crystals a non-linear transition curve^{6,7,9,12,13} is observed. Monte Carlo simulations of the Bose-glass melting⁴ in a vortex system interacting with linear defects gave $\nu \approx 1$ which, through eq. 2, seems to account only for the results in samples with columnar defects. It is therefore important to clarify whether the cusp in samples with planar correlated defects arises as a consequence of a liquid to Bose-glass transition as suggested in ref.⁹, and to which extent the scaling theory describing the vortex dynamics is applicable to this more anisotropic case.

In this paper we show that within the linear regime the scaling hypothesis $\rho(t, \theta) \sim t^{sy} \mathcal{F}_{\pm}(\sin(\theta)t^{-sx})$ is fulfilled for all magnetic fields between 1T and 18T in

YBa₂Cu₃O_{7- δ} heavily oriented-twin single crystals. For all applied fields the transition temperature T_{BG} shows a cusp around $\theta = 0$. However the shape of the $T_{BG}(\theta)$ curve is only consistent with the predictions of Lidmar and Wallin for $H < H^{cr} \approx 4T$. Above this field a change of the cusp's shape is accompanied by a sudden increase in sx from $sx = 1 \pm 0.1$ to $sx = 3 \pm 0.2$ while sy remains constant in the whole field range. This jump of sx is clearly reflected in the scaling of the linear resistivity. We discuss these findings in terms of a change in the universality class of the vortex solid-liquid transition which we ascribe to a corresponding change in the nature of the vortex solid phase as the field is swept through H^{cr} .

The YBa₂Cu₃O_{7- δ} crystal with oriented twins was mounted onto a rotatable sample holder with an angular resolution of $\Delta\theta \approx 0.05^\circ$ inside a cryostat provided with an 18T magnet. The crystal has a critical temperature of $T_c \sim 93\text{K}$ and $\Delta T_c \sim 0.5\text{K}$ width dimension of $1 \times 0.5 \times 0.03\text{mm}^3$. A uniform dc -current was injected through the crystal parallel to the twin planes and the crystal was rotated at angles θ in a plane perpendicular to the twins in a constant Lorentz force configuration (see inset Fig. 1). In this setup the vortices are moved and tilted in a direction perpendicular to the defects. All transport measurements were performed within the linear regime at $J=3\text{Acm}^{-2}$.

In Fig. 1 we show the transition temperature $T_{BG}(\theta)$ for different magnetic fields. This temperature has been defined from $\rho(\theta, T)$ measurements as the temperature at which the data falls below our experimental resolution ($V/I \leq 20\mu\Omega$). The value at $\theta = 0$ coincide within experimental error with that obtained from the scaling of the linear resistivity. It is seen that the shape of the cusp changes as the magnetic field is increased. The change is rather abrupt, and occurs at a crossover field $H^{cr} \approx 4T$. Below H^{cr} the $T_{BG}(\theta)$ is linear in $|\theta|$, while above a non-linear dependence develops. The solid lines, which are fits to eq. 2 with $sx = 1$ for $H= 1\text{T}$ and 2T , and $sx = 3$ for 6T and 8T illustrate this point. The arrows correspond to a critical angle, θ_c , above which the scaling properties of the linear resistivity are lost. Not only the shape of the cusp changes, but its amplitude increases with field. The angular width of the cusp shrinks when the field increases but remains almost constant for $H \geq 4\text{T}$. Interestingly enough, the cusp exists up to the highest magnetic fields we measured (18T). This may be compared to the behavior reported for $T_{BG}(\theta)$ in (Ba,K)BiO₃ irradiated cubic crystals,¹⁰ where the cusp gradually disappears upon surpassing the matching field, B_ϕ , in which the number of vortices equals the number of the columnar defects. The absence of saturation in our experiments indicates that the twin boundary potentials are still efficient to induce vortex confinement and localization in a field range in which induced columnar tracks with $B_\phi \approx 18\text{T}$ would destroy the superconducting properties of the crystal.

The changes in the shape of the phase boundary are also reflected in the dissipation in the liquid state as shown in Fig. 2, in which $\rho(T)$ is plotted for different

angles near $\theta = 0$. Panel (a) shows data characteristic of the low field regime, while panel (b) displays the data corresponding to the high field region. It is worth noticing that the linear dissipation has a different behavior at low and high fields as the angle between the magnetic field and the defects is increased. At low H the $\rho(T)$ curves shift almost parallel to each other while at high fields $\rho(T)$ stretches to lower temperatures as θ is increased. These differences are indicative of a change in the vortex dynamics below and above a crossover field H^{cr} which separates the low and high field regions. In order to quantify the observed changes we refer to the scaling theory^{4,5} according to which the linear resistivity, when the applied field is parallel and vortices move perpendicular to the correlated disorder, should scale as $\rho(T, 0) \sim t^{sy}$ with $sy = \nu(z - 2)$. On the other hand, the resistivity as a function of the tilting angle at the transition temperature should behave as $\rho(0, \theta) \sim \theta^{sy/sx}$ for small angles. These scalings are shown in the insets of panels (a) and (b) for the corresponding fields. In general we find that for $H < H^{cr}$, $sy = 2.4 \pm 0.3$ and $sy/sx = 2.3 \pm 0.2$, while for $H > H^{cr}$ $sy = 2.7 \pm 0.3$ and $sy/sx = 0.9 \pm 0.2$. Note that within experimental error sy seems to be field independent while the ratio sy/sx undergoes an abrupt change. From these we conclude that the changes in the behavior of the linear resistivity are solely due to a change in the exponent sx . In order to see this, we show in Fig. 3 the scaled linear resistivity as predicted by eq. 1. Panel (a) shows the same data displayed in Fig. 2(a), while in panel (b) the scaling of the data in Fig. 2(b) is shown. Both scalings are very good for $\rho(T, \theta)$ curves below the corresponding critical angle θ_c . Curves for $\theta > \theta_c$ do not scale. An important point to note here is that the critical exponent sx is different at low and high fields. In panel (a), $sx = 1 \pm 0.2$ was used to obtain a good scaling, while in panel (b) the value of sx was increased to 3 ± 0.2 in order to make the curves to scale. In the insets the same scaling is shown but forcing the value of sx to be 3 at low fields and 1 at high fields, and maintaining the rest of the parameters constant, as required by consistency with eq. 1 at $\theta = 0$. Clearly, this assignment of critical exponent values renders the scaling impracticable in both cases, indicating that the change in the value sx is outside the errors involved in such scaling. It is worth noticing that an exponent $sx = 1$ corresponds, through eq. 2, to a linear $T_{BG}(\theta)$ dependence, which indeed is seen in Fig. 1 for low fields, while a value of $sx = 3$ gives a non-linear shape as observed in Fig. 1 at high fields.

In Fig. 4 we show a summary of our findings by plotting the values of the two critical exponents and their ratio as a function of the magnetic field. The open circles in panel (a) correspond to the values of sy obtained by a fit of the resistivity data to $\rho(t, 0) \sim t^{sy}$, from which also $T_{BG}(0)$ was obtained. With these values of $T_{BG}(0)$ the scaling of $\rho(t, \theta)$, as required by eq. 1, was performed to obtain the solid squares in panel (a) and (b). The error bars were estimated by the effect the variation of

the exponents s_x and s_y has on the scaling of the linear resistivity. As is seen s_y is, within error bars, independent of the magnetic field and of the way in which it is obtained. The value of s_x , however, jumps from 1 to 3 at 4T, remaining constant for higher or lower fields. Finally in panel (c) we show the ratio of s_y/s_x . The solid squares were calculated from the values in panel (a) and (b) while the open circles were obtained by adjusting the resistivity data at $T_{BG}(0)$ to $\rho(0, \theta) \sim \theta^{s_y/s_x}$. Note that the change at around 4T is independent of the way in which s_y/s_x was obtained.

An important conclusion that can be drawn from our results is that the way in which the linear dissipation in the vortex liquid varies as a function of angle and temperature can be accounted for by a scaling law of the form of eq. 1 independently of the applied magnetic field. This is a fingerprint of a second order vortex solid-liquid phase transition occurring at $T_{BG}(\theta)$ for angles below θ_c . Within this physical picture, our results indicate the existence of two different field regimes characterized each one by different values of the critical exponents which govern the shape of the transition curve and the dynamic response of the liquid phase in the linear regime. On general grounds the two regimes can be interpreted in terms of a change in the universality class to which the solid-liquid transition belongs. Let us first discuss the low field regime.

Our results for $H < H^{cr}$ closely resemble those observed in crystals with columnar defects. We may therefore assume that the $T_{BG}(\theta)$ is linear in $|\theta|$ as a consequence of the interaction of the vortex system with some kind of columnar-type potentials. The identification of the columnar-type defects which might be present in our twinned crystal is however difficult. A possible candidate we found by optical inspection of our crystal were end points of twin planes located between the voltage contacts. An end point breaks the translational symmetry of the twin plane and may emulate a columnar-type defect for vortices located near it. This end point corresponds microscopically to zones where a twin turns into a transverse one, or more likely in a microtwinning region which can not be seen under an optical microscope. Other source of columnar-type defects which can also contribute to localise the vortices in this regime, might be screw dislocations which also exist in twinned $\text{YBa}_2\text{Cu}_3\text{O}_{7-\delta}$ crystals.¹⁴ Within this assumption a matching field should exist, above which all linear defects become occupied by a vortex line. In view of the work of Klein *et al.* showing that the cusp in $T_{BG}(\theta)$ exists up to magnetic fields more than three times larger than the corresponding B_ϕ , it is not straightforward in our case to identify the crossover field H^{cr} with the matching field of the linear defects. It could well be that H^{cr} represents the field above which the effects of the columnar defects are completely washed out. In this case H^{cr} should be sample dependent and could even be absent in crystals of very high quality. This physical picture could be tested in a more direct way by measuring

the vortex transport properties in an oriented-twin crystal with a low concentration of columnar tracks induced by ion irradiation in the c -axis direction.

Once the effect of the columnar potentials has been saturated, the dynamics of the vortex system is determined by its interaction with the twin planes. This corresponds to the field regime above H^{cr} . In this field range vortices localise inside the twin potentials, at $T_{BG}(\theta)$. However, the vortex solid that is formed above H^{cr} ought to be different from that present in samples with columnar tracks alone. A way to see this is to consider the form in which vortices can accommodate inside the correlated potentials. While columnar tracks allow single vortex occupancy only, in a finite sample with twin planes vortices will continue to accommodate inside the correlated defects until the increase in energy due to their mutual interaction overcomes the energy gain due to the vortex-defect interaction. This difference in the way in which vortices interact with and become localised at the twin potentials gives rise to a different dynamical response of the vortex liquid compared to that found in a system interacting with columnar tracks. It is therefore reasonable to conclude that the vortex liquid will freeze in a vortex solid which does not have the same structure as a Bose-glass. The non-linear phase boundary in θ observed in our experiments may be taken as a fingerprint of this novel vortex solid phase. In general we may say that the form of the phase boundary separating the solid and liquid phases is determined by the type of correlated disorder which is present in the sample.

In summary, we have shown that the vortex solid to liquid transition in $\text{YBa}_2\text{Cu}_3\text{O}_{7-\delta}$ oriented-twin crystals is second order within 1T and 18T, and occurs at a phase boundary which is non-linear in angle when the vortex dynamics is dominated by the interaction with planar defects. The linear dissipation in the liquid state in tilted magnetic fields can be very well described by a scaling law theoretically proposed to explain the dynamics of a vortex system interacting with columnar-type pinning potentials, but with different critical exponents. These observations strongly indicate the existence of a distinctly different vortex solid phase in twinned crystals compared to the Bose-glass phase found in samples with columnar defects.

We would like to thank C. Balseiro, and F. de la Cruz for useful comments and discussions. We also thank G. Nieva for providing the oriented-twin crystal and for bringing our attention to ref.¹⁴. Work partially supported by grants from CONICET PIP 4207, and AN-PCyT protect PICT97-03-00061-01116. E. O. is member of CONICET, Argentina.

- ¹ for a review see, G. Blatter *et al.*, Rev. Mod. Phys. **66**, 1125 (1994).
² D. S. Fisher, M. P. A. Fisher, and D. A. Huse, Phys. Rev. B **43**, 130 (1991).
³ D. R. Nelson, and V. M. Vinokur, Phys. Rev. B **48**, 13060 (1993).
⁴ J. Lidmar and M. Wallin, Europhys. Lett. **47**, 494 (1999).
⁵ D. R. Nelson, and V. M. Vinokur, Phys. Rev. B **61**, 5917 (2000).
⁶ T. K. Worthington *et al.*, Physica C **153-155**, 32 (1988).
⁷ S. Fleshler *et al.*, Phys. Rev. B **47**, 14448 (1993).
⁸ W. Jiang *et al.*, Phys. Rev. Lett. **72**, 550 (1994).
⁹ S. A. Grigera *et al.*, Phys. Rev. Lett. **81**, 2348 (1998).
¹⁰ T. Klein *et al.*, Phys. Rev. B **61**, R3830 (2000).
¹¹ A. W. Smith *et al.*, Phys. Rev. Lett. **84**, 4974 (2000).
¹² H. Safar *et al.*, Philos. Mag. B **74**, 647 (1996).
¹³ E. Morr e *et al.*, Phys. Lett. A **233**, 130 (1997).
¹⁴ B. N. Sun, and H. Schmid, J. Cryst. Growth, **100**, 297 (1990).

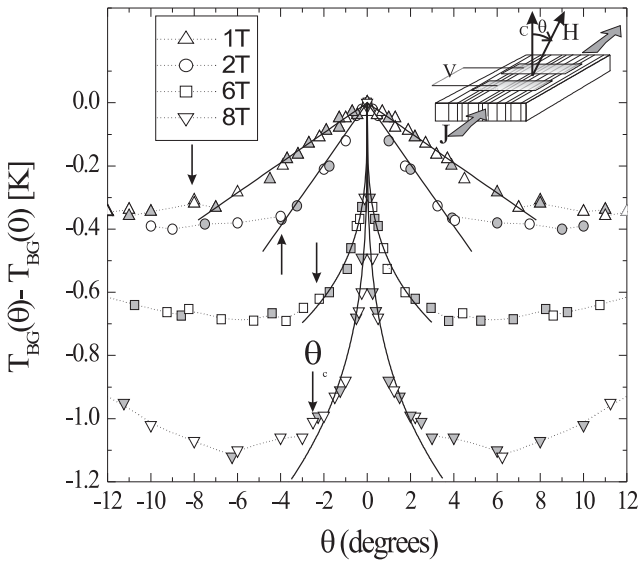


Fig. 1: B. Maiorov and E. Osquiguil

FIG. 1. Angular dependence of $T_{BG}(\theta) - T_{BG}(0)$. Solid lines are fits to eq. 2 with $s_x = 1$ for data at 1T and 2T, and $s_x = 3$ for data at 6 and 8T. The arrows indicate the critical angle θ_c above which the linear resistivity does not scale. Data points are mirrored, gray points correspond to mirrored data. Inset: experimental setup for transport measurements.

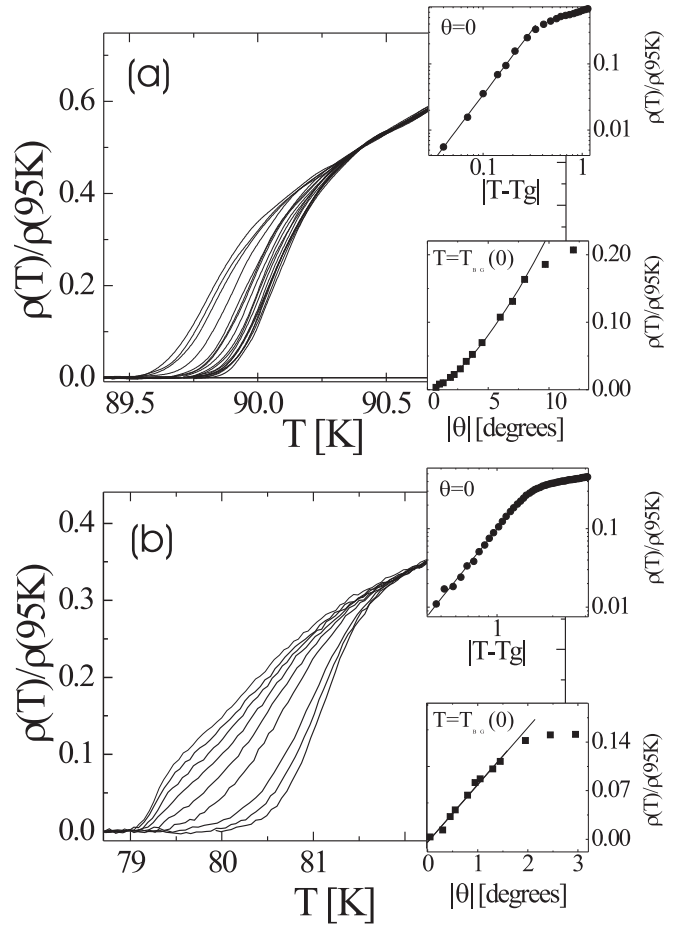


Fig. 2: B. Maiorov and E. Osquiguil

FIG. 2. (a) Normalized resistivity $\tilde{\rho} = \rho/\rho(95K)$ for different tilting angles up to θ_c at $H=1T$, $\theta = 0.2, 0.45, 0.65, 1.0, 1.3, -1.3, 1.6, 1.9, 2.2, 2.7, 3.2, 3.7, -4.5, 6.0, -7.0, 8.0, -8.0$ deg. Upper inset: $\tilde{\rho}(t, 0)$. The solid line is a fit using $\tilde{\rho} \sim t^{s_y}$ with $T_{BG}(0) = (89.82 \pm 0.05)K$ and $s_y = 2.5 \pm 0.3$. Lower inset: $\tilde{\rho}(0, \theta)$. The solid line is a fit to $\tilde{\rho} \sim \theta^{s_y/s_x}$ with $s_y/s_x = 2.2 \pm 0.3$. (b) idem for $H=9T$, $\theta = -0.15, 0.3, 0.75, 0.85, 1.1, 1.25, 1.47, -1.8, 2.25$ degrees. Upper inset: $T_{BG}(0) = (79.85 \pm 0.1)K$ and $s_y = 2.8 \pm 0.3$. Lower inset: $s_y/s_x = 1.1 \pm 0.3$.

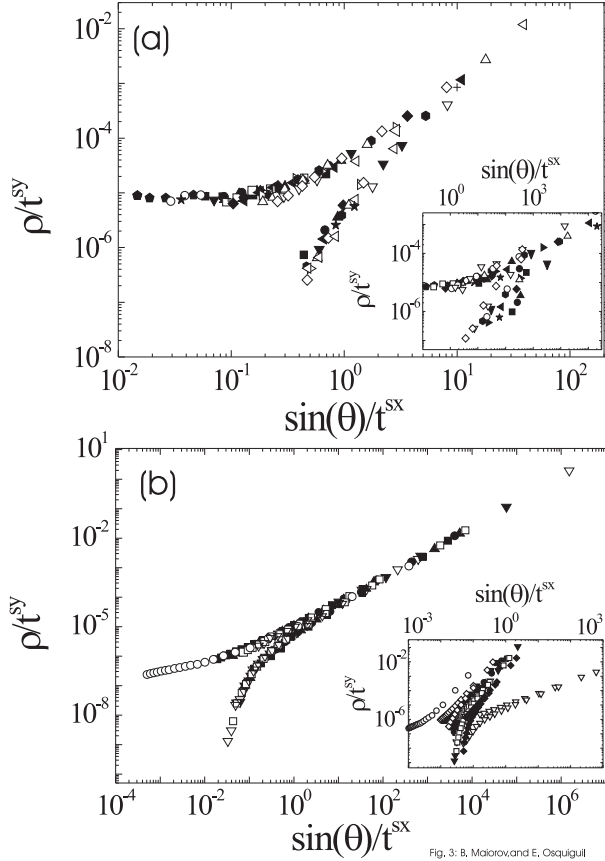


Fig. 3: B. Maiorov and E. Osquiguil

FIG. 3. (a) Scaling of the resistivity curves shown in figure 2(a) according to eq. 1 for $s_y = 2.3$, $s_x = 1.1$ and $T_{BG} = 89.82\text{K}$. The inset shows the same scaling using $s_x = 3$. (b) Scaling of the resistivity curves shown in figure 2(b) according to eq. 1 for $s_y = 2.8$, $s_x = 3.0$ and $T_{BG} = 79.85\text{K}$. The inset shows the same scaling using $s_x = 1$.

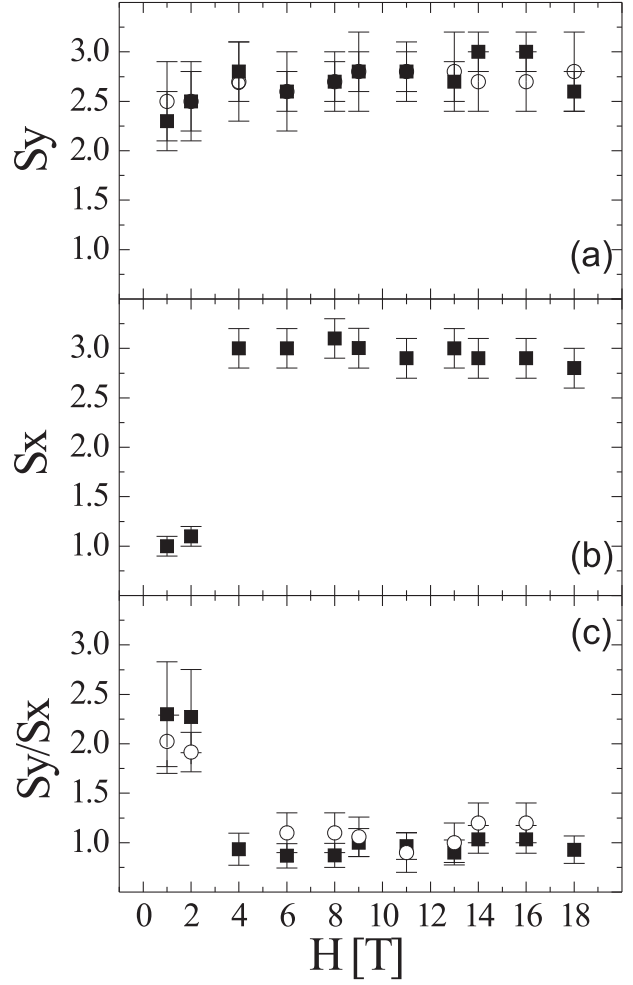


Fig. 4: B. Maiorov and E. Osquiguil

FIG. 4. Summary of the results of the scalings for different fields. (a) Values of s_y according to the resistivity scaling (solid squares) and obtained from $\tilde{\rho}(t, 0) \sim t^{s_y}$ (open circles). (b) Values of s_x according to the resistivity scaling. (c) values of s_y/s_x from the fitting of $\tilde{\rho}(0, \theta)$ (open circles) and the ratio of s_y and s_x obtained from the solid squares in panels (a) and (b).